Annals of Botany **129**: 161–170, 2021
https://doi.org/10.1093/aob/mcab141, available online at www.academic.oup.com/aob

ANNALS OF BOTANY
Founded 1887

Stomatal closure during water deficit is controlled by below-ground hydraulics

Mohanned Abdalla[1,2], Mutez Ali Ahmed[1,3,*], Gaochao Cai[1], Fabian Wankmüller[4], Nimrod Schwartz[5], Or Litig[5], Mathieu Javaux[6,7] and Andrea Carminati[4,*]

[1]Chair of Soil Physics, Bayreuth Center of Ecology and Environmental Research (BayCEER), University of Bayreuth, Bayreuth, Germany, [2]Department of Horticulture, Faculty of Agriculture, University of Khartoum, Khartoum North, Sudan, [3]Department of Land, Air and Water Resources, University of California Davis, Davis, USA, [4]Physics of Soils and Terrestrial Ecosystems, Department of Environmental Systems Science, ETH Zürich, Zürich, Switzerland, [5]Department of Soil and Water Science, The Hebrew University of Jerusalem, Rehovot, Israel, [6]Earth and Life Institute-Environmental Science, Université catholique de Louvain, Louvain-la-Neuve, Belgium and [7]Agrosphere (IBG-3), Forschungszentrum Jülich GmbH, Jülich, Germany
**For correspondence. E-mail Mutez.Ahmed@uni-bayreuth.de or Andrea.Carminati@usys.ethz.ch*

Received: 14 October 2021 Returned for revision: 13 September 2021 Editorial decision: 12 November 2021 Accepted: 16 November 2021
Electronically published: 6 December 2021

• **Background and Aims** Stomatal closure allows plants to promptly respond to water shortage. Although the coordination between stomatal regulation, leaf and xylem hydraulics has been extensively investigated, the impact of below-ground hydraulics on stomatal regulation remains unknown.
• **Methods** We used a novel root pressure chamber to measure, during soil drying, the relation between transpiration rate (E) and leaf xylem water pressure ($\psi_{leaf\text{-}x}$) in tomato shoots grafted onto two contrasting rootstocks, a long and a short one. In parallel, we also measured the $E(\psi_{leaf\text{-}x})$ relation without pressurization. A soil–plant hydraulic model was used to reproduce the measurements. We hypothesize that (1) stomata close when the $E(\psi_{leaf\text{-}x})$ relation becomes non-linear and (2) non-linearity occurs at higher soil water contents and lower transpiration rates in short-rooted plants.
• **Key Results** The $E(\psi_{leaf\text{-}x})$ relation was linear in wet conditions and became non-linear as the soil dried. Changing below-ground traits (i.e. root system) significantly affected the $E(\psi_{leaf\text{-}x})$ relation during soil drying. Plants with shorter root systems required larger gradients in soil water pressure to sustain the same transpiration rate and exhibited an earlier non-linearity and stomatal closure.
• **Conclusions** We conclude that, during soil drying, stomatal regulation is controlled by below-ground hydraulics in a predictable way. The model suggests that the loss of hydraulic conductivity occurred in soil. These results prove that stomatal regulation is intimately tied to root and soil hydraulic conductances.

Key words: *Solanum lycopersicum*, water stress, hydraulic signal, modelling, root system, hydraulic limitations.

INTRODUCTION

Stomata regulate the exchange of carbon and water between the atmosphere and vegetation (Hetherington and Woodward 2003; Wolz *et al.*, 2017; Buckley, 2019; Deans *et al.*, 2020). Stomatal regulation provides a key survival feature to terrestrial vegetation under unfavourable conditions, preventing an excessive drop in water pressure and minimizing the risk of xylem cavitation upon drought (Martin-StPaul *et al.*, 2017; Choat *et al.*, 2018; Grossiord *et al.*, 2020). Despite the importance of this regulation, the mechanisms by which edaphic stress impacts transpiration and stomatal regulation remain elusive.

Stomatal regulation has been extensively studied in relation to xylem vulnerability (Scoffoni *et al.*, 2014; Sperry and Love, 2015; Bartlett *et al.*, 2016; Wolf *et al.*, 2016; Anderegg *et al.*, 2017; Henry *et al.*, 2019; Eller *et al.*, 2020). However, other hydraulic limitations occur along the soil–plant continuum before xylem cavitation (Scoffoni *et al.*, 2017; Huber *et al.*, 2019; Corso *et al.*, 2020; Albuquerque *et al.*, 2020), especially below ground (Rodriguez-Dominguez and Brodribb, 2020; Carminati and Javaux, 2020; Abdalla *et al.*, 2021). For instance, Rodriguez-Dominguez and Brodribb (2020) have recently shown that, in olive trees, the root–soil interface represented the largest hydraulic resistance to water flow. In a follow-up study, Bourbia *et al.* (2021) showed that stomata close concomitantly with the decline in root hydraulic conductivity in both herbaceous and woody species. Abdalla *et al.* (2021) demonstrated that an increase in soil–root hydraulic resistance was the main driver of stomatal closure in tomato. Carminati and Javaux (2020), by means of a soil–plant hydraulic model and a meta-analysis, showed that the loss of soil conductivity, rather than xylem, constrains transpiration. They proposed that stomata close at the onset of hydraulic limitation, i.e. when the relation between transpiration and leaf water potential becomes non-linear (Sperry and Love, 2015; Carminati and Javaux, 2020; see Fig. 1 for details of the main hypothesis). In other words, the loss in soil hydraulic conductance entails severe gradients in soil matric potential around roots, which cause an excessive drop in leaf water pressure to sustain a tiny increment in transpiration. Hence, the relation between stomatal conductance and leaf water potential should be soil- and root-specific (Carminati and Javaux, 2020).

Despite the advances in conceptual and modelling work linking stomatal regulation to soil–plant hydraulics (Sperry and Love, 2015; Wang *et al.*, 2020), there is no conclusive experimental proof that stomatal closure is driven by the loss in below-ground hydraulic conductances (i.e. contrasting root system or soil textures). Previous modelling studies explained midday stomatal closure by the reduction in below-ground hydraulic conductance (Williams *et al.*, 2001; Fisher *et al.*, 2006; Lier *et al.*, 2013). However, these modelling exercises still require experimental validations. Gollan *et al.* (1985, 1986) compared stomatal behaviour of pressurized and unpressurized plants, and showed that stomata close in dry soil conditions even though the shoots were kept turgid. However, Gollan and co-authors did not attempt to link stomatal closure to the onset of the hydraulic non-linearity. We have recently provided the first systematic experimentation to test stomatal sensitivity to the hydraulic non-linearity (Abdalla *et al.*, 2021). We showed that stomatal closure was concomitant with the onset of the non-linearity in $E(\psi_{\text{leaf-x}})$-relation (Abdalla *et al.*, 2021). In this study, we ask the following question: do changes in below-ground traits (i.e. contrasting root system) impact the $E(\psi_{\text{leaf-x}})$ relation during soil drying?

We experimentally tested the hypothesis that below-ground hydraulics, i.e. soil, root and/or their interface, determine the relation between stomatal conductance and leaf water potential. We measured leaf xylem water pressure ($\psi_{\text{leaf-x}}$) and transpiration rate (E) in tomato shoots grafted onto two contrasting rootstocks, a short and a long one. To sustain the same transpiration rate, the short root system would require a larger water flow per root surface, and thus larger gradients in soil matric potential (Fig. 1). Therefore, plants with a shorter root system should exhibit a more marked non-linearity in the $E(\psi_{\text{leaf-x}})$ relation and should close stomata at less negative leaf water pressures (Fig. 1). Alternatively, the larger root system might attenuate the drop in leaf water pressure because of its larger hydraulic capacitance; i.e. not only the ability to conduct water but also the capacity to store water might affect stomatal regulation.

We employed a root pressure chamber designed by Passioura (1980) and implemented by Gollan *et al.* (1986) and recently by Cai *et al.* (2020*a*) to measure the soil–plant hydraulic conductance during soil drying. This method makes it possible to explore the non-linear part of the $E(\psi_{\text{leaf-x}})$ relation. Additionally, we measured transpiration, leaf water pressure (refers to the hydrostatic component of leaf water potential) and root water content during soil drying. The soil–plant hydraulic model of Carminati and Javaux (2020) was used to reproduce and interpret the data.

MATERIALS AND METHODS

Plant preparation

Two tomato varieties with contrasting root lengths were used as rootstocks; *Lycopersicon hirsutum* and a hybrid of *L. hirsutum* and the wild tomato *L. pimpinellifolium* were used as long- and short-rooted plants, respectively. Scions from *Solanum lycopersicum* L. (M82 variety) were grafted onto these two rootstocks. Seeds were provided by Rootility (Israel). Seeds were

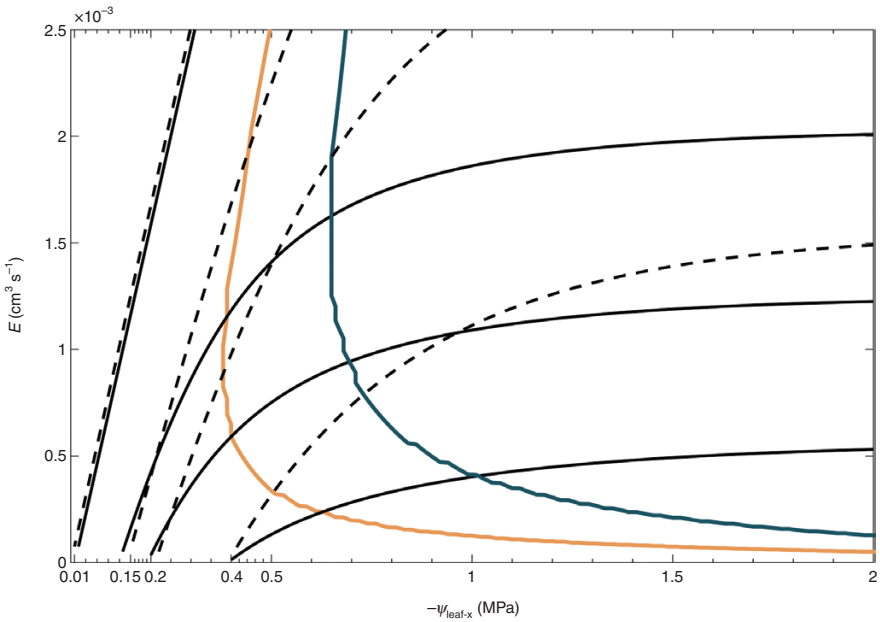

FIG. 1. Hypothesis: reduction in root length causes an earlier drop in soil hydraulic conductance and an earlier stomatal closure. Relation between transpiration (E) and leaf xylem pressure ($\psi_{\text{leaf-x}}$) as simulated by a model of water flow across the soil, the root system and along the xylem, including the non-linearity of their hydraulic conductances (Carminati and Javaux, 2020). The model hypothesizes that stomata close at the onset of hydraulic limitation (stress onset line, SOL), which is defined as the point at which the slope of $E(\psi_{\text{leaf-x}})$ reaches 50 % of its maximum (see Materials and methods and Supplementary Data Table S2). $E(\psi_{\text{leaf-x}})$ relations were simulated at soil matric potentials of –0.01, –0.15 –0.2 and –0.4 MPa. Plants with a short root system (solid black lines and orange SOL) require larger gradients in soil matric potential around their roots, which results in a marked non-linearity in $E(\psi_{\text{leaf-x}})$ compared with plants with a long root system (dashed lines and blue SOL). Consequently, stomatal closure occurs at less negative $\psi_{\text{leaf-x}}$ for plants with short root systems (orange line for the short and blue line for the long root system).

sown in polyvinyl chloride (PVC) columns 30 cm in height and 10 cm in diameter. The columns had five holes with a diameter of 5 mm on the side to facilitate soil moisture content measurements. The PVC columns were topped (using a silicon rubber glue; Teroson, Henkeln, Germany) with a 0.8-cm-thick aluminium plate that had a centred hole 1.4 cm in diameter.

Plants were grafted ~1 week after germination when their stem diameters were matching (Notaguchi *et al.*, 2020). Immediately after grafting, plants were placed inside a chamber at ~95 % relative humidity and 200 µmol m^{-2} s^{-1} photosynthetic photon flux density (PPFD) for 4 d to avoid scion desiccation (Rosskopf *et al.*, 2018). Thereafter, plants were placed in a climate-controlled room with a day/night temperature of 28/18 °C, a day/night relative humidity of 57/65 %, 14-h photoperiod and PPFD of 600 µmol m^{-2} s^{-1} during the daytime (Luxmeter PCE-174, Meschede, Germany).

After 12 d, plants were moved to the laboratory and sealed at the collar using glue (Uhu Plus Endfest 300, Bühl, Germany). During the experiments, leaves were imaged to determine leaf area (LA; cm^2) using ImageJ 1.50e (http://imagej.nih.gov/ij). After the experiments, roots were washed and root length was measured using WinRihzo (Regent Instruments, Canada). Supplementary Data Fig. S1 shows root length and leaf area.

Soil preparation

A sandy loam soil was used in the experiments. Quartz sand and loamy soil were sieved through a 1-mm sieve. The sieved substrates were mixed in the ratio of 62.5 % loamy soil and 37.5 % quartz sand. The soil water content (θ [cm^3 cm^{-3}]) was measured using a time-domain refractometer (TDR) (E-Test, Lublin, Poland). The hydraulic properties of the soil mixture were determined via a Hyprop system (UMS, Munich, Germany), which implemented the evaporation method. The water retention curve and the unsaturated hydraulic conductivity were fitted using the Peters–Durner–Iden (PDI) model (Peters *et al.*, 2015). The corresponding parameters were estimated by fitting the measured soil matric potential and solving the Richards equation.

Transpiration and leaf xylem water pressure measurements

We used a novel root pressure chamber system (RPCS) to simultaneously measure transpiration (E) and leaf xylem water pressure ($\psi_{leaf\text{-}x}$) within an intact plant (Cai *et al.*, 2020*a*). The construction and calibration of the RPCS were recently described in Cai *et al.* (2020*b*). Briefly, RPCS is composed of a pressure chamber topped with a cuvette and a control unit. Four groups of light-emitting diode (LED) lamps were vertically attached to the cuvette. The lamps provided PPFD that ranged adjustably from 0 to 1000 µmol m^{-2} s^{-1}. We altered E by changing PPFD, and the latter was measured via a fixed radiometric sensor (Gamma Scientific, San Diego, USA). A constant airflow passed through the cuvette (8.25 L min^{-1}) and a fan was used to stir the air inside. Combined temperature–humidity sensors (Galltec-Mela, Bondorf, Germany) continuously measured the temperature and the relative humidity of the inward and the outward air. We determined E by multiplying the airflow by the difference between the outward and the inward humidity. Canopy conductance was calculated as $g_c = (E/\mathrm{LA})/(\mathrm{VPD}/P_{atm})$ according to Jarvis and McNaughton (1986), where VPD is vapour pressure deficit and P_{atm} is atmospheric pressure.

The basic principle of the method was to balance the negative water pressure inside the plant by applying a pneumatic pressure to the soil and root system, thereby bringing water inside the leaf xylem to atmospheric pressure (Passioura, 1980; Carminati *et al.*, 2017; Cai *et al.*, 2020*a*) (Supplementary Data Fig. S2). The applied pressure (balancing pressure; P) is numerically equal to leaf xylem tension before pressurization (Passioura, 1980). A meniscus system was connected to a leaf cut to evaluate the stability of the droplet. We determined $\psi_{leaf\text{-}x}$ when the meniscus was stable for ~10 min (Cai *et al.*, 2020*a*).

To measure $E(\psi_{leaf\text{-}x})$ relation, plants were positioned inside the RPCS, with the column inside the pressure chamber and the shoot inside the cuvette. We modified E by gradually increasing PPFD from 0 to 200, 400, 600, 800 and 1000 µmol m^{-2} s^{-1}. Simultaneously, the corresponding $\psi_{leaf\text{-}x}$ was determined at each PPFD. Additionally, E was also measured without pressurization at 1000 µmol m^{-2} s^{-1}. Canopy conductance (g_c [mol m^2 s^{-1}]) was calculated from E without pressurization. Each plant was measured for several days during soil drying (Supplementary Data Fig. S3 and Table S1).

In parallel, we measured $\psi_{leaf\text{-}x}$ at the highest E for unpressurized plants using a leaf pressure chamber (Soil Moisture Equipment Corp., Santa Barbara, CA, USA) as described in Scholander *et al.* (1965). These measurements were utilized to assess $\psi_{leaf\text{-}x}$ values obtained from pressurized plants at the same values of E and θ (Abdalla *et al.*, 2021).

Osmotic potential

Leaf osmotic potential was measured using a vapour pressure osmometer (VAPRO, Wescore). Xylem sap was collected from a leaf cut using a 10-µL pipette after applying 0.1 MPa more than the balancing pressure. Leaf osmotic potential was measured at different soil matric potentials during soil drying. Soil osmotic potential was measured when the soil was saturated.

Root hydraulic capacitance

Root hydraulic capacitance was obtained by measuring the root water content at decreasing soil matric potentials. Plants from both rootstock genotypes were grown in the sandy loam. When individuals reached targeted soil matric potential, plants were left overnight inside a humid chamber (relative humidity ≈100 %) to allow soil and roots to equilibrate to the same water pressure. Roots were carefully removed from the soil and were gently shaken to remove any attached soil, and initial fresh weight was measured. Root dry weight was obtained after drying the roots for 24 h at 105 °C. The difference between fresh and dry weights of the roots was divided by their dry weight at different soil matric potentials to calculate root hydraulic capacitance (see eqn 15).

Soil–plant hydraulic model

We used a soil–plant hydraulic model to simulate the water flow in the soil–plant continuum and fit the measured $E(\psi_{\text{leaf-x}})$ relation. Water flow was modelled through a series of resistances across the soil, across the soil–root interface, across the root to the root xylem, and along the xylem. We briefly describe the model here.

The Buckingham–Darcy law, ignoring gravity, was used to describe the radial water flow in soil towards the root surface:

$$q = -K_s(\psi_m)\frac{\partial \psi_m}{\partial r} \quad (1)$$

where q is the water flux (cm s^{-1}), K_s is the soil hydraulic conductivity, which is a function of the soil matric potential ψ_m (hPa), r is the radial distance (cm) and $\partial\psi_m/\partial r$ is the gradient in matric potential. Note that when the soil matric potential is expressed in unit heads (cm, 1 hPa ≈ 1 cm), K_s has units of cm s^{-1}. We use this unit throughout the text when describing soil water flow.

The boundary conditions were expressed as follows:

$$q(r_0) = \frac{E}{2\pi r_0 L} \quad (2)$$

$$q(r_b) = 0 \quad (3)$$

where r_0 and r_b are the root radius and the exterior radius of soil around the root (cm), E is the transpiration rate (cm^3 s^{-1}) and L is the root length active in water uptake (cm); r_b is determined by L and the volume of the column V (cm^3), according to:

$$r_b = \sqrt{\frac{V}{\pi L}} \quad (4)$$

We parameterized K_s according to the Brooks and Corey model:

$$K_s(\psi_m) = K_{sat}\left(\frac{\psi_m}{\psi_0}\right)^{\tau} \quad (5)$$

where K_{sat} is the saturated hydraulic conductivity of the soil (cm s^{-1}), ψ_0 is the soil air entry value (cm) and τ is a fitting parameter (−). We obtained the parameters for eqn (5) by matching the PDI and Brooks and Corey models (Abdalla *et al.*, 2021). According to de Jong van Lier *et al.* (2008), and assuming a steady-rate behaviour for the water flow in the soil, the radial geometry of water flow could be reformulated using the matric flux potential (Φ, cm^2 s^{-1}):

$$\Phi(\psi) = \int_{-\infty}^{\psi_m} K(x)\,dx \quad (6)$$

The solution of eqn (6) describes the matric flux potential at the outer boundary $r = r_b$:

$$\Phi_{soil} = \frac{k_{sat}.{\psi_m}^{1-\tau}.{\psi_0}^{-\tau}}{1-\tau} \quad (7)$$

where Φ_{soil} is the matric flux potential in the bulk soil (cm^2 s^{-1}) corresponding to the measured bulk soil matric potential (ψ_m).

Meanwhile, the radial flow could be described by combing eqns (1, 5 and 6) as:

$$q = -\frac{\partial \varnothing\,(\psi_m)}{\partial r} \quad (8)$$

We obtain the flux boundary condition at the soil–root interface, Φ_{root_soil} (cm^2 s^{-1}), by combining eqns (5 and 6) and the radial Richards equation (Schröder *et al.*, 2009):

$$\Phi_{root\_soil} = -\frac{E}{2\pi L}\left(\frac{1}{2} - r_b^2\frac{\ln(r_b/r_0)}{r_b^2 - r_0^2}\right) + \frac{k_{sat}\cdot{\psi_m}^{1-\tau}\cdot{\psi_0}^{-\tau}}{1-\tau} \quad (9)$$

The water flow in the root is given by

$$E = -K_{root}\left(\psi_{root\_xylem} - \psi_{root\_soil}\right) \quad (10)$$

where E is the water flow in the root equal to the transpiration rate (cm^3 s^{-1}), ψ_{root_soil} is the water potential at the root–soil interface (here converted to MPa, 1 MPa ≈ 10^4 cm), ψ_{root_xylem} is the water potential at the xylem collar (MPa) and K_{root} (cm^3 s^{-1} MPa^{-1}) is the root hydraulic conductance. Note that differences in osmotic potential between soil and root xylem can occur and affect the driving force of water flow across the root–soil interface. Therefore, ψ_{root_soil} and ψ_{root_xylem} are the sum of their respective matric/hydrostatic potentials and osmotic potentials. Doing so, we assume that the reflection coefficient of the root is 1. The difference between leaf and soil osmotic potential is equal to the measured difference between soil matric potential and leaf xylem pressure when water flow is negligible (Cai *et al.*, 2020*a*).

We assume no further change in osmotic potential along the xylem. The xylem conductance, K_x (cm^3 s^{-1} MPa^{-1}), which includes the effect of cavitation, is given by:

$$K_x = K_{root}\left(\frac{\psi_{leaf\text{-}x}}{\psi_{0x}}\right)^{-\tau_x} \quad (11)$$

where $\psi_{leaf\ -x}$ is the leaf xylem pressure (MPa), ψ_{0x} is the xylem pressure (MPa) at which K_x drops and τ_x is a fitting parameter (−) that determines the rate of this drop.

The plant conductance, K_{plant} (cm^3 s^{-1} MPa^{-1}), is given by the harmonic mean of K_{root} and K_x:

$$\frac{1}{K_{plant}} = \frac{1}{K_{root}} + \frac{1}{K_x} \quad (12)$$

The leaf matric flux potential is calculated as:

$$\Phi_{leaf} = -E + \Phi_{root\_xylem} \quad (13)$$

Leaf xylem pressure $\psi_{leaf\ -x}$ is calculated by inserting K_x into eqn (6) and combining eqns (11 and 13):

$$\psi_{leaf\_x} = \left({\psi_{root\_xylem}}^{1-\tau_x} - \frac{E\,(\tau_x - 1)}{{\psi_{0x}}^{\tau_x}\,K_{root}}\right)^{\frac{1}{1-\tau_x}} \quad (14)$$

Note that the unit of the matric flux potentials in eqn (13) differs from those of eqn (9) because soil and xylem hydraulic conductivities have different units.

Data were firstly fitted for each day of measurements (i.e. at each measured soil water content) individually to estimate K_{root}, L and the offset between soil matric potential and leaf xylem pressure. Inverse simulations revealed that L increased as soil dries (reported and discussed later). Therefore, we conducted direct simulations for each group of plants allowing the parameter L to vary during soil drying. We obtained K_{root} from individual simulations by fitting the linear part of the $E(\psi_{leaf\text{-}x})$ relation, which was constant during soil drying (Abdalla *et al.*, 2021).

The onset of hydraulic limitation is defined as the point at which the slope of $E(\psi_{leaf\text{-}x})$ reaches 50 % of its maximum (the soil matric potential being kept constant: soil isolines) (Carminati and Javaux, 2020). Note that the 50 % is rather arbitrary and indeed a value between 40 and 60 % would give the same shape of the stress onset line (SOL). The maximum slope of $E(\psi_{leaf\text{-}x})$ at any given soil matric potential is at null transpiration; i.e. the slope of $E(\psi_{leaf\text{-}x})$ decreases with increasing E (Carminati and Javaux, 2020).

The model was used (1) to predict the onset of hydraulic limitation and compare it with measurements of transpiration reduction, and (2) to test whether the decline of $E(\psi_{leaf\text{-}x})$ is explained by the loss of soil hydraulic conductivity for the two root systems.

Soil–plant hydraulic model including root capacitance

The model above assumed that all water transpired was taken up from the soil (no changes in root water content) and that the change in soil water content during one measurement cycle was negligible. The calculated $E(\psi_{leaf\text{-}x})$ lines were referred to as soil isolines. The consequence of these assumptions was tested by including measurements of root capacitance and soil drying in the model. We examined to what extent root capacitance attenuates the decline in soil and leaf water potential during one measurement cycle consisting of increasing transpiration rates over a period of ~6 h. The rationale is that root capacitance diminishes the water uptake from the soil. This leads to more water remaining in the soil and a less negative leaf water potential to sustain transpiration.

Root capacitance and soil drying were modelled during one exemplary measurement cycle. The relation between root water content and water potential was obtained by fitting the measured gravimetric root water content θ_g, defined as weight of water in the root divided by root dry weight. The volumetric root water content θ_{root} was calculated based on densities of water and roots ρ_{H_2O} and ρ_{wet}:

$$\theta_{root} = \theta_g * \frac{\rho_{wet}}{\rho_{H_2O}} \quad (15)$$

where ρ_{wet} is the dry root weight divided by the volume of the wet root. The water flow resulting from root shrinkage is the time derivative of the root water volume. This flow was subtracted from the transpiration rate to obtain the root water uptake. To do so, soil matric potential and root water content were estimated for each time step. We simulated two scenarios: (1) soil drying but no root capacitance; and (2) soil drying and root capacitance. The two scenarios were compared with two isolines calculated using the steady-state soil–plant hydraulic model described in the paragraph above (no root capacitance and no changes in soil water content). We calculated one isoline corresponding to the soil matric potential at the beginning of the measurement cycle (fitted to the first two points) and one soil isoline corresponding to the soil matric potential at the end of the measurement cycle (fitted with the last measurement).

Statistical analysis

We used a mixed model to analyse the influence of root system, soil water content, PPFD and their interactions on E using analysis of variance. Replicates were taken as random factors and the remaining parameters were taken as fixed factors. Furthermore, we tested the values of stomatal closure in $E(\psi_{leaf\text{-}x})$ of the two rootstocks using analysis of covariance. MATLAB 2019a (9.6.0., Mathworks®) was used to perform the statistical analysis.

RESULTS AND DISCUSSION

Tomato plants were grafted on two contrasting root systems to evaluate the impact of root length on soil–plant hydraulic conductance and stomatal regulation during soil drying. The length of the two root systems differed by a factor of 3 ($P < 0.05$), whereas root diameter and leaf area were similar ($P > 0.05$; Supplementary Data Fig. S1).

The relationship between transpiration rates (E) and leaf xylem water pressure ($\psi_{leaf\text{-}x}$) varied between the two root systems (Fig. 2). $E(\psi_{leaf\text{-}x})$ was linear in wet soils ($\theta \geq 0.15$), with the slope being equal to the plant hydraulic conductance. The relation became non-linear as the soil dried (Fig. 2). The long root system sustained higher E during soil drying, while a more marked non-linearity in $E(\psi_{leaf\text{-}x})$ appeared in the short root system at relatively high $\psi_{leaf\text{-}x}$ and soil water content (θ). Longer roots ensured the linearity of $E(\psi_{leaf\text{-}x})$ for a broader range of E and θ.

The $\psi_{leaf\text{-}x}$ of pressurized and unpressurized plants, for the same values of E and θ, matched well (Fig. 3, $r^2 = 0.81$). This result demonstrates that the total hydraulic conductances of pressurized and unpressurized plants were similar, which is consistent with Abdalla *et al.* (2021). Note that pressurization maintained the water pressure in the xylem equal to the atmospheric pressure and hence cavitation did not occur during the measurements. Additionally, pressurized plants had a turgid shoot, whose conductivity is likely to have remained constant during the measurements. The latter is in line with the finding of Skelton *et al.* (2017), who showed a decline in leaf hydraulic conductance when leaf water potential dropped beyond −1.28 MPa in tomato. Further, we used roots of *L. hirsutum* and its hybrid with the wild tomato *L. pimpinellifolium*, which might potentially have more resistant xylem. Therefore, the non-linearity of $E(\psi_{leaf\text{-}x})$ must have been caused by a decline in the below-ground hydraulic conductivity, either in the soil, in the root system or at their interface.

The $E(\psi_{leaf\text{-}x})$ and $E(\psi_{soil})$ relations were well reproduced by the soil–plant hydraulic model of Carminati and Javaux (2020) (black lines in Fig. 4A–D). The model calculates the water potential gradients across the soil–plant continuum based on the measured transpiration rates, soil water content and soil

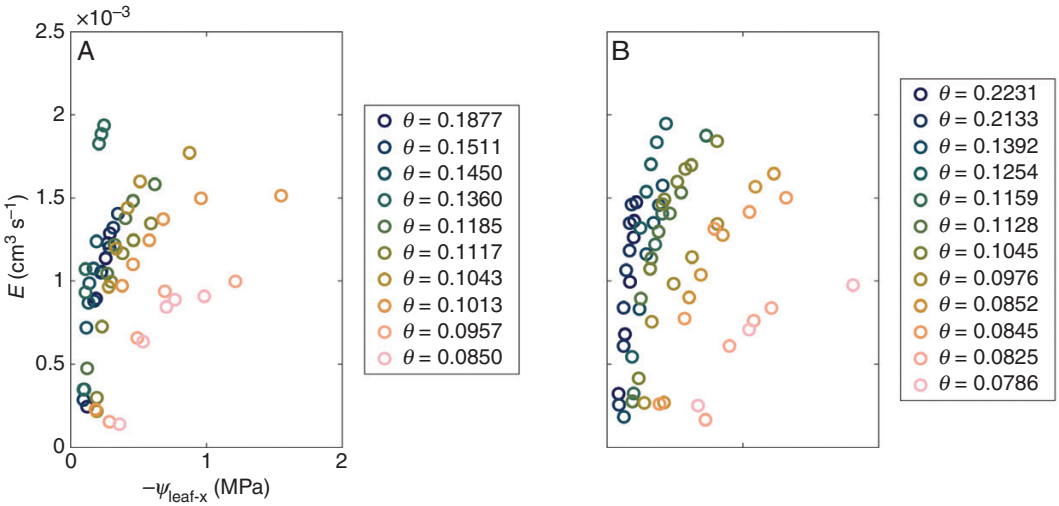

FIG. 2. Measured relation between transpiration (E) and leaf xylem pressure ($\psi_{leaf\text{-}x}$) in tomato plants grafted onto (A) a short root system and (B) a long root system during soil drying (θ: soil water content [$cm^3\ cm^{-3}$], $N = 6$).

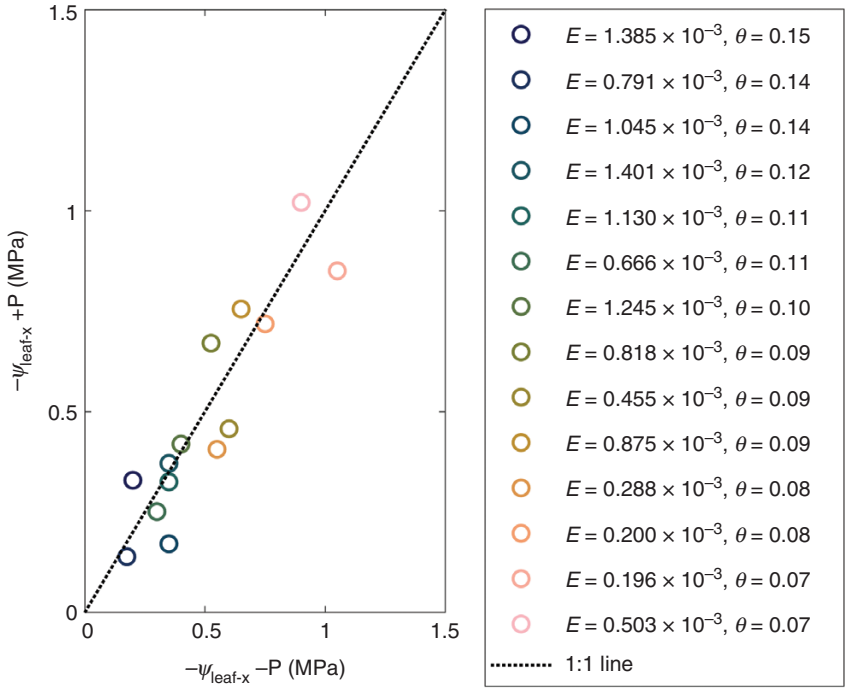

FIG. 3. Leaf xylem pressure ($\psi_{leaf\text{-}x}$) in pressurized (+P) and unpressurized (−P) tomato plants at the same soil water content (θ [$cm^3\ cm^{-3}$]) and transpiration rate (E [$cm^3\ s^{-1}$]). The $\psi_{leaf\text{-}x}$ of pressurized plants was measured by the RPCS, while $\psi_{leaf\text{-}x}$ of unpressurized plants was measured with a Scholander leaf pressure chamber ($N = 6$). The $\psi_{leaf\text{-}x}$ of pressurized and unpressurized plants, for the same values of E and θ, matched well ($r^2 = 0.81$).

hydraulic properties (see the Materials and methods section and Supplementary Data Table S2 for details of the model description and parameters). The fitting parameters were the root length active in root water uptake L, which was allowed to vary with soil drying, root conductance K_{root}, and xylem water pressure at which xylem conductivity drops. The latter was set to −1.5 MPa, which is the most negative value measured in the experiments, and thus does not affect the simulations. This choice was based on the observation that pressurized and non-pressurized plants had the same hydraulic conductance, which means that cavitation did not affect the plant hydraulic conductance. The model reproduced well the experimental observation that a more marked non-linearity in the $E(\psi_{leaf\text{-}x})$ relation occurred in the short root system (Fig. 4E).

The measurements of soil and leaf xylem osmotic potential are consistent with the offset between soil matric potential

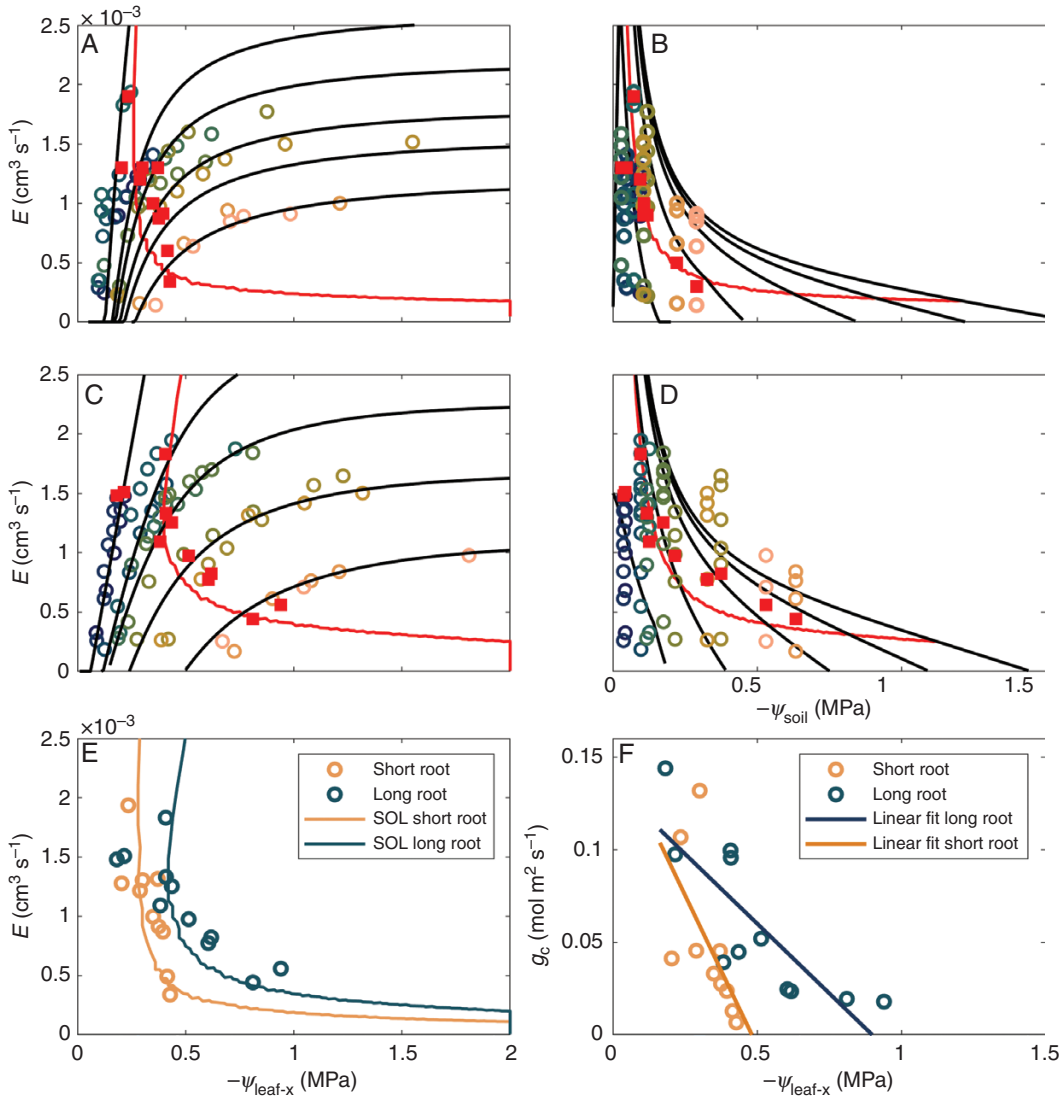

FIG. 4. Relation between transpiration rate (E) and leaf xylem pressure ($\psi_{\text{leaf-x}}$) (A, C) as well as predawn leaf xylem pressure ($\psi_{\text{leaf-x-PD}}$) as proxy of soil matric potential (ψ_{soil}) (B, D), for the short (A, B) and long (C, D) root systems. The measurements (open symbols) were well reproduced by the model (black lines) at different soil water contents (different colours). The relation shifted from linear to non-linear during soil drying. The red line marks the onset of non-linearity (SOL). The red squares in (A–D) are the measured transpiration rates during soil drying in unpressurized plants (short root system, $r^2 = 0.74$, 0.72; long root system, $r^2 = 0.82$, 0.78 from leaf and soil views, respectively). (E) Onset of hydraulic limitation (SOL) for long-rooted (blue line) and short-rooted plants (orange line) match well the reduction in transpiration (blue and orange open symbols, respectively). The reduction in transpiration of long- and short-rooted plants was significantly different ($P < 0.001$; Supplementary Data Fig. S4), with the shorter root system reducing transpiration at less negative $\psi_{\text{leaf-x}}$. (F) Canopy conductance (g_c) as a function of $\psi_{\text{leaf-x}}$ for the short-rooted (orange open symbols) and long-rooted plants (blue open symbols). The slope and the intercept of the linear fit were used for the analysis of covariance, which showed a significant difference in stomatal closure between the two root systems ($P < 0.01$).

and predawn leaf xylem pressure. Soil osmotic potential was around −0.02 MPa at soil saturation. This supports the interpretation that the offset was caused by the difference in osmotic potentials. No visible differences were observed between the osmotic potentials of the two root systems, possibly also due to the variability in the measurements (Fig. 5A).

The simulations predict the active root length L as a function of the ψ_{soil} (Fig. 5B). The simulated active root length L was greater in the plants with the long root system. The explanation is that a longer root length requires a lower flow rate of water at the root–soil interface and smaller gradients in soil matric potential to sustain the same transpiration rate. The simulations support the hypothesis that the non-linearity in the $E(\psi_{\text{leaf-x}})$ relation is mainly caused by soil hydraulics. Interestingly, active root length increased as the soil dried, which might be a mechanism to compensate limited fluxes per root segment. The increase in L during soil drying was also observed in maize (Cai *et al.*, 2021) and might reflect root hydraulic adjustment to soil drying. However, L has to be interpreted with caution; L is a fitting parameter and might reflect oversimplification of the plant–soil hydraulic model, such as the representation of the root system with a single root and the assumption that the rhizosphere has the same hydraulic conductivity as the bulk soil.

An alternative explanation of the better ability of the long root system to sustain transpiration during soil drying could

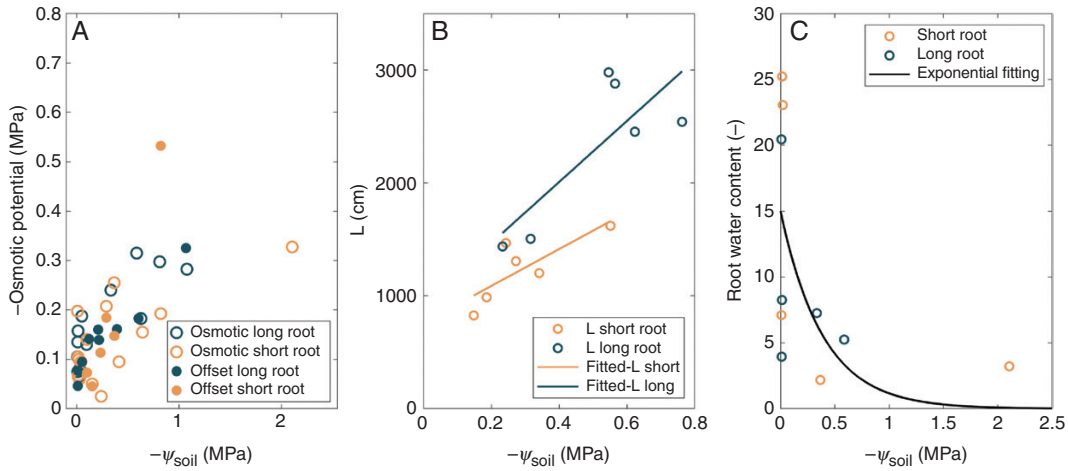

FIG. 5. (A) Model predictions of the leaf xylem osmotic potential matched the direct measurements of leaf osmotic potential in both root systems (as indicated in the key) during soil drying. (B) Active root length (L) as a function of soil matric potential (ψ_{soil}) for short-rooted and long-rooted plants (as indicated in the key). Longer-rooted plants had more active roots, especially in the dry range of ψ_{soil}. (C) The difference between root fresh and dry weight was divided by dry weight to obtain root shrinkage. Root water content decreased exponentially as soil matric potential declined.

be the effect of root capacitance. We investigated the effect of root capacitance by including in the simulations the measured decrease in root water content at decreasing soil matric potential (Fig. 5C). The simulated trajectories of plants with and without root capacitance (green and pink) were very close, indicating that root capacitance had a minor contribution to $E(\psi_{leaf\text{-}x})$ (Fig. 6). By contrast, the decrease in soil water content during a measurement cycle had significant effects. To understand the effect of decreasing soil water content during a measurement cycle, we plotted the soil isolines at the initial and final stages (orange and blue) of the measurement cycle using the steady-state model. The two isolines perfectly envelop the measurements using a root length of 4000 cm, which is 2.5 times longer than the value estimated using a single line to simulate all points of the measurement cycle ($L = 1496$ cm). The difference in L shows the problems in using the isolines to fit the data and interpret L as the active root length. The isoline would predict a shorter root length than the actual value, and this mismatch is caused by neglecting the decrease in soil water content. In contrast, the potential role of root capacitance in buffering the decline of soil and leaf water potentials was negligible. However, the choice against specific model simplifications (root shrinkage, rapid soil drying) must match with the research questions addressed. For example, to predict the onset of non-linearity, the classical model approach with soil isolines (solid black line in Fig. 6) is acceptable. However, to reproduce the leaf water potential measurements and properly estimate the active root length, simulations should include the role of soil drying. In summary, the model simulations reinforce the explanation that the drop in soil conductivity is the main cause of non-linearity in the soil–plant system.

The onset of hydraulic non-linearity (SOL) was defined as the point when the slope of $E(\psi_{leaf\text{-}x})$ decreased down to 50 % of its maximum (Carminati and Javaux, 2020). The SOL matches well with the transpiration rate of unpressurized plants (Fig. 4A–E). This supports the idea that stomata close when the relation between transpiration rate and leaf water potential becomes non-linear, as hypothesized by Sperry and Love (2015) and Carminati and Javaux (2020).

The measured $E(\psi_{leaf\text{-}x})$ relation as well as the SOL of the long and short root systems differed (Fig. 4E), which supports our hypothesis (Fig. 1). Analysis of covariance shows that stomatal closure was significantly different between the two root systems without pressurization ($P < 0.001$, Fig. 4F; Supplementary Data Fig. S4 and Tables S3 and S4). Plants with a short root system reached 50 % transpiration at $\psi_{leaf\text{-}x} = -0.3$ MPa compared with $\psi_{leaf\text{-}x} = -0.5$ MPa with the long root system (Fig. 4E).

Taken together, the measured relations between transpiration rate and leaf water pressure proved that stomata close at the onset of hydraulic non-linearity, as hypothesized in previous models (Sperry and Love, 2015; Carminati and Javaux, 2020). Additionally, the measurements show that a decrease in root length induces an earlier non-linearity in the soil–plant hydraulic conductance and triggers an earlier stomatal closure, which supports our hypothesis (Fig. 1).

We conclude that the relation between stomatal conductance and leaf water potential is affected by root length and below-ground hydraulics, particularly soil hydraulic conductance. This finding has important implications for understanding and predicting the response of transpiration to drought. So far, the current trend puts the focus on the coordination between stomatal closure and xylem vulnerability (Wolf *et al.*, 2016; Anderegg *et al.*, 2017; Henry *et al.*, 2019; Eller *et al.*, 2020). However, to properly predict stomatal closure and understand its relation to soil–plant hydraulics, root length, root and soil hydraulic conductivities are essential. Our results show a tied link between soil hydraulic conductivity, active root length and stomatal conductance, and the coordination between these variables is central in predicting the ability of plants to cope with water shortage. Further research would be needed to explore variations between plant species growing in contrasting soil textures and climatic conditions.

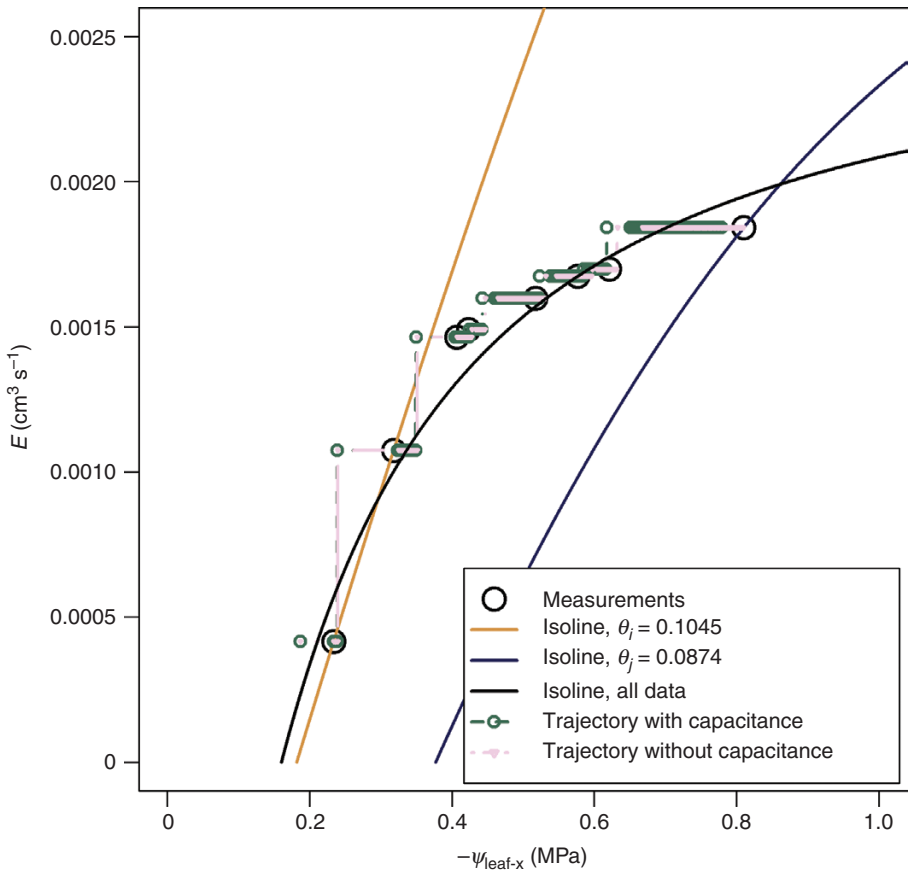

FIG. 6. Relation between transpiration rate (E) and leaf xylem pressure ($\psi_{\text{leaf -x}}$) for one exemplary measurement cycle ($\theta = 0.1045$). Different model simulations were compared regarding their explanatory values. The measurements were well captured by a single soil isoline fitted to all data points (as indicated in the key) using the steady-state soil–plant hydraulic model. To understand the effect of decreasing soil water content during the measurement cycle, we plotted the soil isolines at the initial ($\theta_i = 0.1045$) and final ($\theta_j = 0.0874$) soil water content of the measurement cycle using the steady-state model but with different fitting parameters (L and K_{root}) compared with the single soil isoline. The simulated trajectories with and without root capacitance were very close, indicating that root capacitance had a minor contribution to the $E(\psi_{\text{leaf -x}})$ relation. Both trajectories reproduced the measurements very well.

SUPPLEMENTARY DATA

Supplementary data are available at *Annals of Botany* online and consist of the following. Figure S1: root length and leaf area of tomato plants grafted onto two root systems. Figure S2: the root pressure chamber system used to measure the relation between transpiration and leaf xylem water pressure. Figure S3: transpiration rate of plants with short and long root systems during soil drying. Figure S4: linear fit of the $E(\psi_{\text{leaf-x}})$ relation measured in unpressurized plants with the two root systems. Table S1: analysis of variance for the influence of different factors on the transpiration rate under plant pressurization. Table S2: parameters used in the model. Table S3: coefficient estimates for stomatal closure $E(\psi_{\text{leaf-x}})$ in the two rootstocks in terms of the slope and the intercept. Table S4: analysis of variance to identify the significant difference between the slope and the intercept of $E(\psi_{\text{leaf-x}})$.

FUNDING

The doctoral position of M.A. was funded by Deutscher Akademischer Austauschdienst (DAAD, the German Academic Exchange Servic). The position of G.C. was founded by Bundesministeriums für Bildung und Forschung (BMBF, the Federal Ministry of Education and Research), Project 02WIL1489 (Deutsch-Israelische Wassertechnologie-Kooperation).

ACKNOWLEDGEMENTS

M.A., M.A.A., G.C. and A.C. designed the experiments. M.A. performed the experiments and wrote the first draft. M.A., F.W. and A.C. made the simulations. M.A.A., G.C., M.J. and A.C. contributed to the writing. N.S. and O.L. provided the seeds and contributed to the study design. All authors discussed the results and approved the final version.

LITERATURE CITED

Abdalla M, Carminati A, Cai G, Javaux M, Ahmed MA. 2021. Stomatal closure of tomato under drought is driven by an increase in soil-root hydraulic resistance. *Plant, Cell & Environment* **44**: 425–431.

Albuquerque C, Scoffoni C, Brodersen CR, Buckley TN, Sack L, McElrone AJ. 2020. Coordinated decline of leaf hydraulic and stomatal conductances under drought is not linked to leaf xylem embolism

for different grapevine cultivars. *Journal of Experimental Botany* **71**: 7286–7300.

Anderegg WRL, Wolf A, Arango-Velez A, *et al.* 2017. Plant water potential improves prediction of empirical stomatal models. *PLoS ONE* **12**: e0185481.

Bartlett MK, Klein T, Jansen S, Choat B, Sack L. 2016. The correlations and sequence of plant stomatal, hydraulic, and wilting responses to drought. *Proceedings of the National Academy of Sciences of the USA* **113**: 13098–13103.

Bourbia I, Pritzkow C, Brodribb TJ. 2021. Herb and conifer roots show similar high sensitivity to water deficit. *Plant Physiology* **186**: 1908–1918.

Buckley TN. 2019. How do stomata respond to water status? *New Phytologist* **224**: 21–36.

Cai G, Ahmed MA, Dippold MA, Zarebanadkouki M, Carminati A. 2020*a*. Linear relation between leaf xylem water potential and transpiration in pearl millet during soil drying. *Plant and Soil* **447**: 565–578.

Cai G, Ahmed MA, Reth S, Reiche M, Kolb A, Carminati A. 2020*b*. Measurement of leaf xylem water potential and transpiration during soil drying using a root pressure chamber system. *Acta Horticulturae* **1300**: 131–138.

Cai G, Carminati A, Abdalla M, Ahmed MA. 2021. Soil textures rather than root hairs dominate water uptake and soil-plant hydraulics under drought. *Plant Physiology* **187**: 858–872.

Carminati A, Javaux M. 2020. Soil rather than xylem vulnerability controls stomatal response to drought. *Trends in Plant Science* **25**: 868–880.

Carminati A, Passioura JB, Zarebanadkouki M, *et al.* 2017. Root hairs enable high transpiration rates in drying soils. *New Phytologist* **216**: 771–781.

Choat B, Brodribb TJ, Brodersenx CR, Duursma RA, López R, Medlyn BE. 2018. Triggers of tree mortality under drought. *Nature* **558**: 531–539.

Corso D, Delzon S, Lamarque LJ, *et al.* 2020. Neither xylem collapse, cavitation, or changing leaf conductance drive stomatal closure in wheat. *Plant, Cell & Environment* **43**: 854–865.

Deans RM, Brodribb TJ, Busch FA, Farquhar GD. 2020. Optimization can provide the fundamental link between leaf photosynthesis, gas exchange and water relations. *Nature Plants* **6**: 1116–1125.

Eller CB, Rowland L, Mencuccini M, *et al.* 2020. Stomatal optimization based on xylem hydraulics (SOX) improves land surface model simulation of vegetation responses to climate. *New Phytologist* **226**: 1622–1637.

Fisher RA, Williams M, Do Vale RL, Da Costa AL, Meir P. 2006. Evidence from Amazonian forests is consistent with isohydric control of leaf water potential. *Plant, Cell & Environment* **29**: 151–165.

Gollan T, Turner NC, Schulze E-. 1985. The responses of stomata and leaf gas exchange to vapour pressure deficits and soil water content: III. In the sclerophyllous woody species *Nerium oleander*. *Oecologia* **65**: 356–362.

Gollan T, Passioura JB, Munns R. 1986. Soil water status affects the stomatal conductance of fully turgid wheat and sunflower leaves. *Australian Journal of Plant Physiology* **13**: 459–464.

Grossiord C, Buckley TN, Cernusak LA, *et al.* 2020. Plant responses to rising vapor pressure deficit. *New Phytologist* **226**: 1550–1566.

Henry C, John GP, Pan R, *et al.* 2019. A stomatal safety-efficiency trade-off constrains responses to leaf dehydration. *Nature Communications* **10**: 1–9.

Hetherington AM, Woodward FI. 2003. The role of stomata in sensing and driving environmental change. *Nature* **424**: 901–908.

Huber AE, Melcher PJ, Piñeros MA, Setter TL, Bauerle TL. 2019. Signal coordination before, during and after stomatal closure in response to drought stress. *New Phytologist* **224**: 675–688.

Jarvis PG, McNaughton KG. 1986. Stomatal control of transpiration: scaling up from leaf to region. In: MacFadyen A, Ford ED, eds. *Advances in ecological research, Vol. 15*. London: Academic Press, 1–49.

de Jong van Lier Q, van Dam JC, Metselaar K, de Jong R, Duijnisveld WHM. 2008. Macroscopic root water uptake distribution using a matric flux potential approach. *Vadose Zone Journal* **7**: 1065–1078.

de Jong van Lier Q, van Dam JC, Durigon A, dos Santos MA, Metselaar K. 2013. Modeling water potentials and flows in the soil–plant system comparing hydraulic resistances and transpiration reduction functions. *Vadose Zone Journal* **12**: vzj2013.02.0039.

Martin-StPaul N, Delzon S, Cochard H. 2017. Plant resistance to drought depends on timely stomatal closure. *Ecology Letters* **20**: 1437–1447.

Notaguchi M, Kurotani KI, Sato Y, *et al.* 2020. Cell-cell adhesion in plant grafting is facilitated by β-1,4-glucanases. *Science* **369**: 698–702.

Passioura JB. 1980. The transport of water from soil to shoot in wheat seedlings. *Journal of Experimental Botany* **31**: 333–345.

Peters A, Iden SC, Durner W. 2015. Revisiting the simplified evaporation method: identification of hydraulic functions considering vapor, film and corner flow. *Journal of Hydrology* **527**: 531–542.

Rodriguez-Dominguez CM, Brodribb TJ. 2020. Declining root water transport drives stomatal closure in olive under moderate water stress. *New Phytologist* **225**: 126–134.

Rosskopf E, Pisani C, Di Gioia F. 2018. Crop-specific grafting methods, rootstocks and scheduling-tomato. In: Kubota C, Miles C, Zhao X, eds. Grafting Manual: How to Produce Grafted Vegetable Plants. SCRI Vegetable Grafting Org., 1–13.

Scholander PF, Bradstreet ED, Hemmingsen EA, Hammel HT. 1965. Sap pressure in vascular plants: negative hydrostatic pressure can be measured in plants. *Science* **148**: 339–346.

Schröder T, Javaux M, Vanderborght J, Körfgen B, Vereecken H. 2009. Implementation of a microscopic soil–root hydraulic conductivity drop function in a three-dimensional soil–root architecture water transfer model. *Vadose Zone Journal* **8**: 783–792.

Scoffoni C, Vuong C, Diep S, Cochard H, Sack L. 2014. Leaf shrinkage with dehydration: coordination with hydraulic vulnerability and drought tolerance. *Plant Physiology* **164**: 1772–1788.

Scoffoni C, Albuquerque C, Brodersen CR, *et al.* 2017. Outside-xylem vulnerability, not xylem embolism, controls leaf hydraulic decline during dehydration. *Plant Physiology* **173**: 1197–1210.

Skelton RP, Brodribb TJ, Choat B. 2017. Casting light on xylem vulnerability in an herbaceous species reveals a lack of segmentation. *New Phytologist* **214**: 561–569.

Sperry JS, Love DM. 2015. What plant hydraulics can tell us about responses to climate-change droughts. *New Phytologist* **207**: 14–27.

Wang Y, Sperry JS, Anderegg WRL, Venturas MD, Trugman AT. 2020. A theoretical and empirical assessment of stomatal optimization modeling. *New Phytologist* **227**: 311–325.

Williams M, Bond BJ, Ryan MG. 2001. Evaluating different soil and plant hydraulic constraints on tree function using a model and sap flow data from ponderosa pine. *Plant, Cell & Environment* **24**: 679–690.

Wolf A, Anderegg WR, Pacala SW. 2016. Optimal stomatal behavior with competition for water and risk of hydraulic impairment. *Proceedings of the National Academy of Sciences of the USA* **113**: E7222–E7230.

Wolz KJ, Wertin TM, Abordo M, Wang D, Leakey ADB. 2017. Diversity in stomatal function is integral to modelling plant carbon and water fluxes. *Nature Ecology & Evolution* **1**: 1292–1298.